Proceedings of the 18th International Conference on Nuclear Engineering
ICONE18
May 17-21, 2010, Xi`an, China

ICONE18-29545

CHARACTERISTICS OF CAVITATION AND EROSION PHENOMENA IN SODIUM FLOW

Teddy Ardiansyah*
Department of Nuclear Engineering
Tokyo Institute of Technology
2-12-1-N1-18, O-okayama, Meguro-ku,
Tokyo, 152-8550, Japan
+81-3-5734-2957, +81-3-5734-2959(fax)
ardiansyah.t.aa@m.titech.ac.jp

Makoto Asaba
Sukegawa Electric Co., Ltd.
3-19-5, Namekawahontyo, Hitachi,
Ibaraki, 317-0051, Japan
asaba@net-sukegawa.com

Kuniaki Miura
Sukegawa Electric Co., Ltd.
3-19-5, Namekawahontyo, Hitachi,
Ibaraki, 317-0051, Japan
asaba@net-sukegawa.com

Minoru Takahashi
Research Laboratory for Nuclear Reactors
Tokyo Institute of Technology
2-12-1-N1-18, O-okayama, Meguro-ku,
Tokyo, 152-8550, Japan
+81-3-5734-2957, +81-3-5734-2959(fax)
mtakahas@nr.titech.ac.jp

ABSTRACT

This paper presents experimental data of cavitation experiments to determine the characteristics of cavitation and erosion in the flowing liquid sodium at 200-400°C. The test section is a venturi made from SUS316 since this material is used as the cladding material for SFR. The ID and OD of the venturi test section are 6.5 mm and 21.4 mm, respectively. The data show that the onset cavitation conditions (onset velocities) in liquid sodium are influenced by the change of the stagnant pressure at the expansion tank. Cavitation noise signals at developed cavitation conditions are not affected by the change of stagnant pressure and might be caused by choking of the sodium flow that restricts the formation of cavitation bubbles. For all the different stagnant pressures and temperatures, the onset cavitation coefficient K is around unity. Meanwhile, erosion experiment in the flowing liquid sodium for 600 hours at 200°C and cavitation coefficient value K of 0.59-0.51 (developed cavitation condition) reveals that cavity bubbles produce some micro pits at the outlet of the venturi test section. These pits indicate that erosion is occurred on the surface of the tested material and could be a major problem for the development of SFR if cavitation occurs inside the critical/important parts.

1. INTRODUCTION

Research on cavitation is one of the key issues to ensure the safety in the design of sodium-cooled fast reactor (SFR). The influences are classified into fluid-dynamic, mechanical, and core neutronics performances as follows: the occurrence of cavitation affects fluid-dynamic performances of flow regulating mechanisms in inner structure of reactor vessel; the collapse of cavitation bubbles produces shock waves which in turn damage the edges of orifices and change the flow rate distribution in the core; the shock waves could also damage the structural materials and piping walls; vibrations due to cavitation cause metal fatigue of piping systems; and the entry of cavitation bubbles into the core causes instability of core reactivity.

Meanwhile, in the development of more economic SFR, reactor vessels and flow components are made compact which lead to fast flow of reactor coolant. This fast flow could create cavity bubbles due to reduction of liquid's static pressure below

its vapor pressure. And the collapse of cavity bubbles will erode the surface of the material.

Cavitation erosion researches in liquid metal coolants have been investigated by several authors in the past using venturi or vibratory test apparatuses, such as by Thiruvengadam, Preiser and Rudy [1], Hattori *et al* [2], Garcia and Hammitt [3], Young and Johnson [4], and Belahadji, Franc and Michel [5]. However, most of the data obtained are for short time scales and longer time scales have not been investigated in detail. Therefore, more data are needed in longer time scales in order to investigate the effect of cavitation on material erosion.

In this study, cavitation erosion in liquid metal coolant was investigated for longer time scale (600 hours) in venturi test section made of SUS316. Moreover, the characteristics of cavitation (onset conditions and acoustics noise signals) in liquid sodium are also discussed.

2. EXPERIMENTAL APPARATUS

2.1. Description of Sodium Loop

Liquid sodium cavitation experiment was conducted using a sodium loop facility at Sukegawa Electric Co., Ltd. shown in Fig. 1. This sodium loop facility can be operated up to 500°C. The physical and thermodynamics properties of sodium are listed in Tab. 1. The loop consists of a test section, an electromagnetic pump (EMP), two electromagnetic flow rate meters (EMFs), a heater, a cooler, a cold trap and an expansion tank. The heater and expansion tank control the temperature and the stagnant pressure of the sodium loop at the required experimental conditions, respectively. Argon gas was used as cover gas inside the expansion tank. The flow rate of the liquid sodium was measured using the EMF at the bottom part of the loop. The cold trap and EMF-2 are shown by the green lines.

Table 1. Physical and thermodynamics properties of sodium.

Melting point [°C]	98
Boiling point [°C]	883
Liquid density at 200°C [kg/m^3]	903
Vapor pressure at 200°C [Pa]	2.391x10^{-3}

Table 2. Chemical composition of SUS316.

Material	%
Mn	2.00
Si	1.00
S	0.03
P	0.045
Cr	16-18
Ni	10-14

2.2. Description of the Test Section

Figure 2 shows the test section of the liquid sodium cavitation experiment. The test section of the loop is made from SUS316 since this material is used as fuel cladding in SFR. The chemical composition of SS316 is shown in Tab. 2. It consists of a gas injector (30% of porosity), a venturi, a wave guide rod and a static pressure tap. A gas injector is assembled at the upstream of the test section to inject argon gas in the flowing liquid sodium, although it was not used in the present experiment. The venturi part of the test section was used to create cavitation bubbles when liquid sodium flowing thorough this part due to the decrease of the local static pressure. The inner diameter (ID) and the outer diameter (OD) of this part are 6.5 mm and 21.4 mm, respectively. The acoustics noise signals generated from the cavitation bubbles were measured by using an accelerometer (Ono Sokki NP-2710) installed at the bottom part of the wave guide rod. The static pressure of the liquid sodium downstream of the test section was measured by the diaphragm connected at the pressure tap and transmitted along the silicon oil tube to the pressure transducer (Ashcroft GC-51). This silicon oil tube also acts as a heat resistance to keep the maximum allowable temperature of the pressure gauge below 200°C, as shown in Fig. 3.

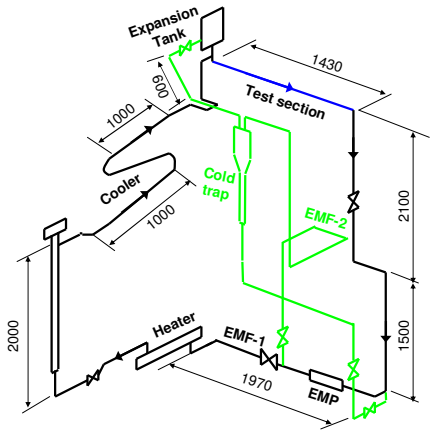

Figure 1. Schematic of the sodium loop facility.

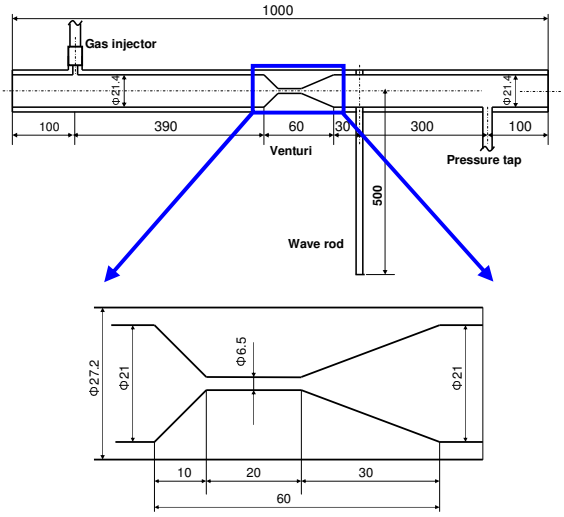

Figure 2. Liquid sodium test section part.

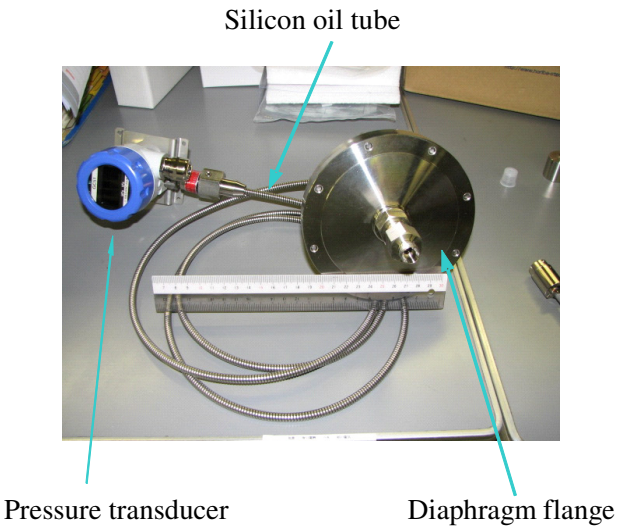

Figure 3. Photograph of diaphragm type pressure gauge.

3. EXPERIMENTAL PROCEDURE

The experiments were conducted at sodium stagnant pressure inside the expansion tank of 0.06-0.18 MPa-a (MPa absolute) and temperature of 200-400°C. The detailed experimental procedures can be explained as follows:

1) At the beginning, the loop was circulated with a desired level of experimental temperature.
2) The EMP was turned off. Then, the pressure at the expansion tank was controlled to a desired level of experimental conditions by injecting argon gas.
3) When the experimental conditions were all reached, the EMP was turned on again to circulate the liquid sodium.
4) The EMP voltage was increased gradually to the desired cavitation conditions and the experimental data were collected.

For liquid sodium cavitation erosion experiment, the liquid sodium temperature was kept at 200°C. The argon gas pressure at the expansion tank and the flow rate of liquid sodium were controlled at 0.05-0.1 kgf/cm^2 and 27-28 L/min, respectively. These values correspond to cavitation coefficient K of 0.59-0.51 (developed cavitation condition). This cavitation condition is kept for 600 hours. After the experiment, the venturi part of the test section was cut and washed by alcohol and water to remove the sodium. Then the surface of the test section was analyzed.

4. RESULTS AND DISCUSSIONS

4.1. Characteristics of Cavitation

The cavitation coefficient K in this experiment is derived from the Bernoulli`s equation for incompressible flow.

$$P_1 + \frac{\rho}{2} V_1^2 = P_0 + \frac{\rho}{2} V_0^2 \tag{1}$$

If P_1 is close to the saturation pressure P_v of the liquid, then the cavitation coefficient K can be expressed as

$$K = \frac{P_0 - P_v}{\frac{\rho}{2}\left(V_1^2 - V_0^2\right)} \tag{2}$$

and for $V_1 >> V_0$

$$K \approx \frac{P_0 - P_v}{\frac{\rho}{2} V_1^2} \tag{3}$$

According to the theory, cavitation starts to occur when cavitation coefficient K is equal to unity. Therefore, it could be used as a prediction of cavity bubbles formation.

The results of the cavitation experiment in flowing liquid sodium are presented in Figs. 4 to 13 and based on authors' work in reference [6]. Figures 4 and 5 show the result of the acoustic noise intensity over cavitation coefficient K at 300° and 400°C. The results show that the noise intensity is relatively low when there is no cavitation in the venturi region (K is higher than unity). The noise intensity begins to rise rapidly when K approaches unity (onset of cavitation). Under developed cavitation condition (K is lower than unity), the noise intensity is relatively stable without changing drastically. The change of the stagnant pressure at the expansion tank has no significant effect on the noise intensity in developed cavitation conditions. The noise intensity at 400°C has no significant differences with that at 300°C, which is around 43 dB. The onset cavitation condition is judged by hearing the rapid knocking sound of cavitation on the cavitation test section and observing the spectrum analyzer monitor for any changes of the noise amplitude signals. We conclude that cavitation starts to occur (onset of cavitation) when there is a sudden increase on the amplitude of the acoustic noise signal, and rapid knocking sounds in the test tube. The judgment of the onset condition could not be done directly by observing the growth of cavity bubbles since sodium is opaque.

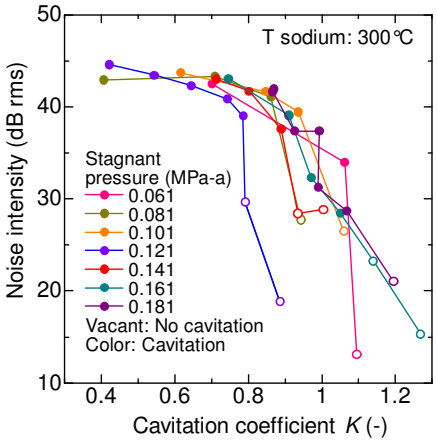

Figure 4. Noise intensity vs cavitation coefficient at 300°C.

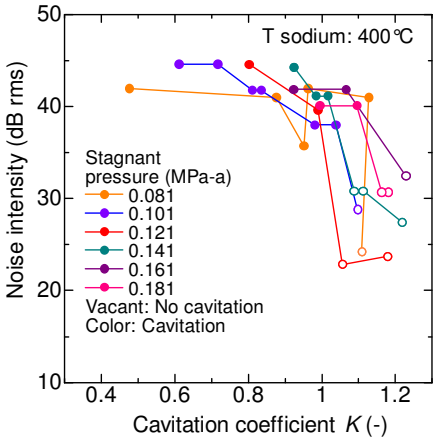

Figure 5. Noise intensity vs cavitation coefficient at 400°C.

Figures. 6, 7 and 8 show the results of no cavitation and occurrence of cavitation on the map of the venturi velocity (superficial velocity of liquid sodium at venturi part of the test section) vs cavitation coefficient at 200°, 300° and 400°C, respectively. For every temperature rise, it is clear that the stagnant pressure in the expansion tank has influence on the onset cavitation velocity at the venturi part. The superficial velocity of liquid sodium at the venturi increases with the increase of the stagnant pressure conditions. The velocity becomes relatively stable in the developed cavitation conditions. Cavitation coefficient at the onset cavitation condition was nearly equal to unity. However, an increase in temperature shifts the cavitation coefficient to a value a little higher than unity. From these figures it can be concluded that the formation of the cavitation bubbles is suppressed at higher stagnant pressure, therefore the onset cavitation velocity in the venturi increases as predicted from eq. (3). It is noted also from the figures that there are two distinct regions, the no cavitation region (K>1), and the cavitation region (K<1).

These figures also show that if the cavitation coefficient is below unity; the sodium superficial velocity at the venturi is relatively constant. This is similar to the choked flow phenomenon. In the choked flow phenomenon, the decrease in the downstream pressure below a certain level of critical pressure does not significantly increase the flow rate. For cavitation in a venturi, the choked flow phenomenon is caused by the decrease of the sound velocity in the liquid sodium due to the formation of cavitation bubbles.

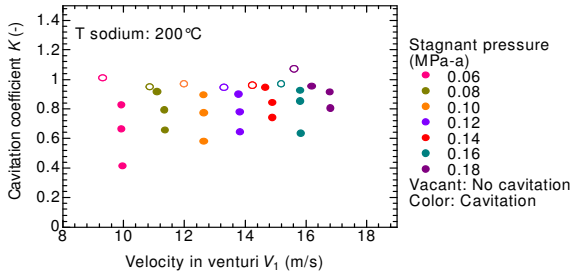

Figure 6. Cavitation coefficient K vs venturi velocity at 200°C.

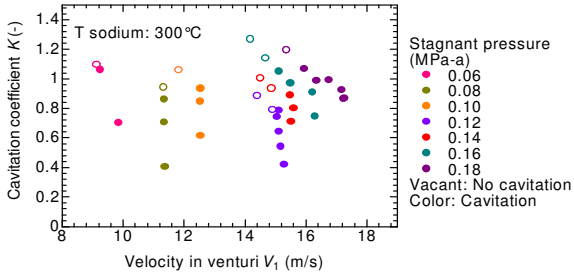

Figure 7. Cavitation coefficient K vs venturi velocity at 300°C.

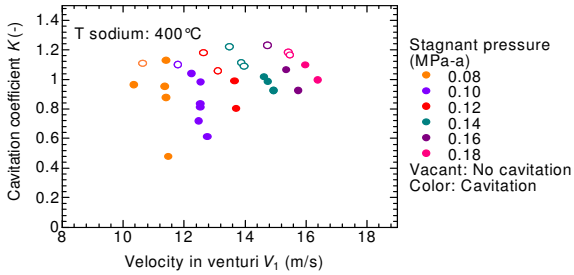

Figure 8. Cavitation coefficient K vs venturi velocity at 400°C.

Figure 9 shows the resonance frequency of the test section at 200°C, 0.12 MPa-a and the flow rate of liquid sodium in the loop is zero. This figure is obtained from hitting the test section by hammer several times until some resonance peaks occur. The resonance frequencies of the test section are indicated by the peaks of noise intensity around 1000, 3000, 5000, 9000, and 20,000 Hz as shown in Fig. 9. The noise intensities have the

significant increase in the high frequency regions than in the low frequency regions.

Figures 10 and 11 show the noise intensity spectrum at different stagnant pressure conditions at 200°C. The results show a significant increase of noise when cavitation bubbles formed at the venturi. At no cavitation conditions, the noise intensity at the higher frequencies is relatively lower compared to that at the lower ones. At developed cavitation conditions, the noise intensity is relatively unchanged. This might be caused by the relatively constant formation and collapse of cavitation bubbles due to choking condition. In the Figs. 10 and 11, the change of the stagnant pressure in the expansion tank from 0.06 to 0.18 MPa-a does not have significant effect on the magnitude of the noise intensity at developed cavitation. It can be concluded that the magnitude of cavitation noise intensity at 200°C is independent of the stagnant pressure change. These figures also show some resonance peaks similar with those obtained in Fig. 9.

Figure 12 show the results at 300°C. The results at 300°C are almost similar with those at 200°C. The similar resonance peaks can also be seen clearly at 300°C as in 200°C.

Result at 400°C is shown in Fig. 12. At 400°C, the noise intensities are unstable at developed cavitations based on hearing the noise sounds and observing the spectrum at computer monitor. We find that sometimes the magnitude of the noise intensity is large (similar to the noise generated by the developed cavitation conditions) for a relatively long time, but then the noise becomes relatively low (similar to the noise generated by the no cavitation conditions). These instabilities of the noise intensities are probably caused by the increasing amount of cavitation bubbles due to the higher vapor pressure. Further examinations are needed to understand the cause of these instabilities at high temperature (400°C).

From the data obtained at 200°, 300°, and 400°C, we conclude that the stagnant pressure change at the expansion tank does not affect the magnitude of the noise intensity at developed cavitations for 200°, 300°, and 400°C. Therefore, it is independent of the stagnant pressure level. While the onset of cavitation bubbles is affected by the stagnant pressure change.

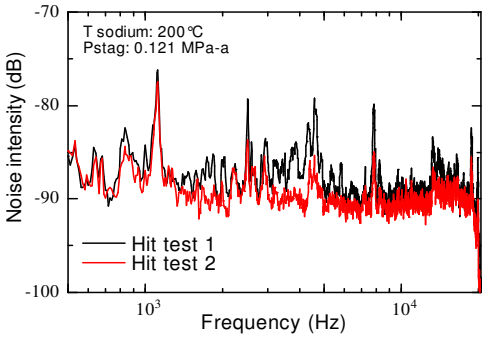

Figure 9. Resonance frequency of the test section.

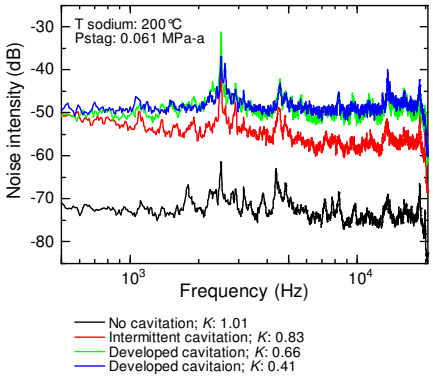

Figure 10. Noise intensity spectrum at 200°C and 0.06 MPa-a.

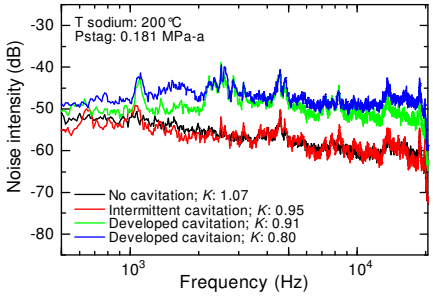

Figure 11. Noise intensity spectrum at 200°C and 0.18 MPa-a.

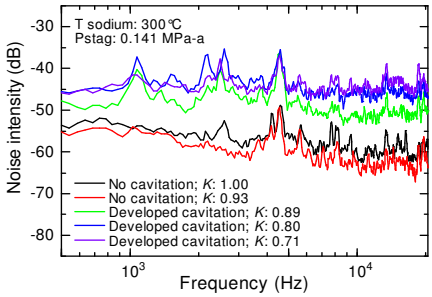

Figure 12. Noise intensity spectrum at 300°C and 0.14 MPa-a.

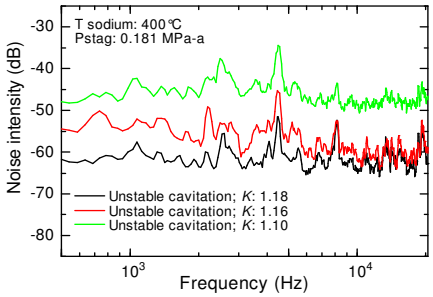

Figure 13. Noise intensity spectrum at 400°C and 0.08 MPa-a.

4.2. Cavitation Erosion of SUS316

Figure 14 shows the test section part after cavitation erosion experiment for 600 hours. The venturi part of the test section was cut into half and the cross section was polished smoothly (Fig. 14b) to observe the eroded part from the boundary of the test section. However, it is very difficult to observe the eroded part caused by cavitation from its cross section. Observation by using X-ray on the venturi test section (Fig. 14c) reveals no major damage on the material's surface caused by intensive collapse of cavity bubbles for 600 hours. Major damage such as large crack that causes sodium leak is undesirable in the operation of SFR. This leak will cause fire if the liquid sodium is in contact with atmospheric air such as the case in Monju accident.

Observation of the material's surface after erosion test was conducted by using optical micrograph. This result can be seen in Fig. 15. The surface of the material at the inlet part of the venturi (upper photo of Fig. 15) reveals relatively smooth surface. No clear micro pits are observed at this region. At this region, cavity bubbles are formed when the liquid sodium flowing into the venturi part. Lower photo of Fig. 15 shows the outlet part of the venturi. The surface shows some pitting damage. This damage is caused by the collapse of cavitation bubbles when travelling out from the venturi. The collapse produces shock waves which impinge on the surface, hence creating some observable micro pits. From Fig. 15 it can be stated that although no major damage is observed on the test section for 600 hours but some pits are formed at the outlet of the test section. These pits are indications that erosion is occurred on the surface.

(a)

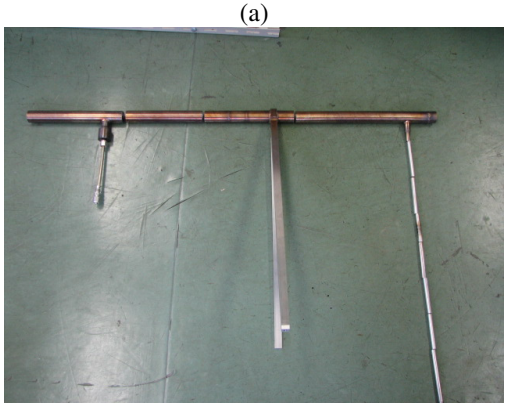

(b)

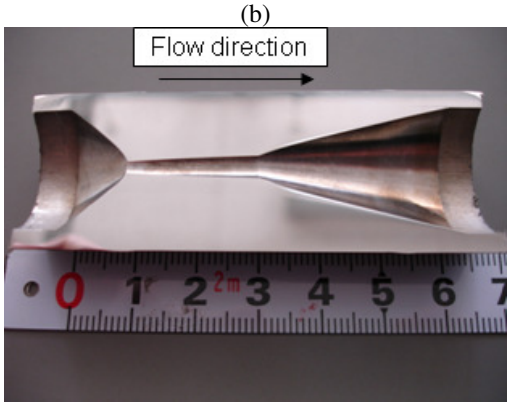

(c)

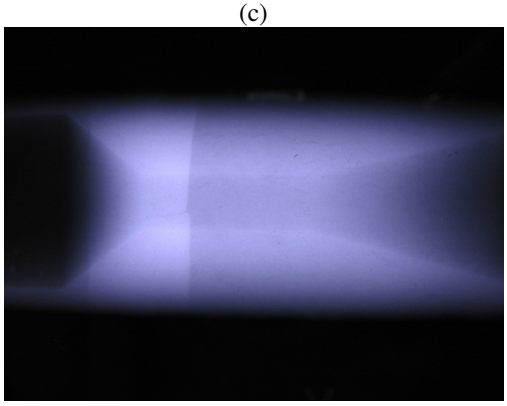

Figure 14. a) Cavitation test section after erosion test; b) venturi part of the test section; c) X-ray photograph of the venturi part.

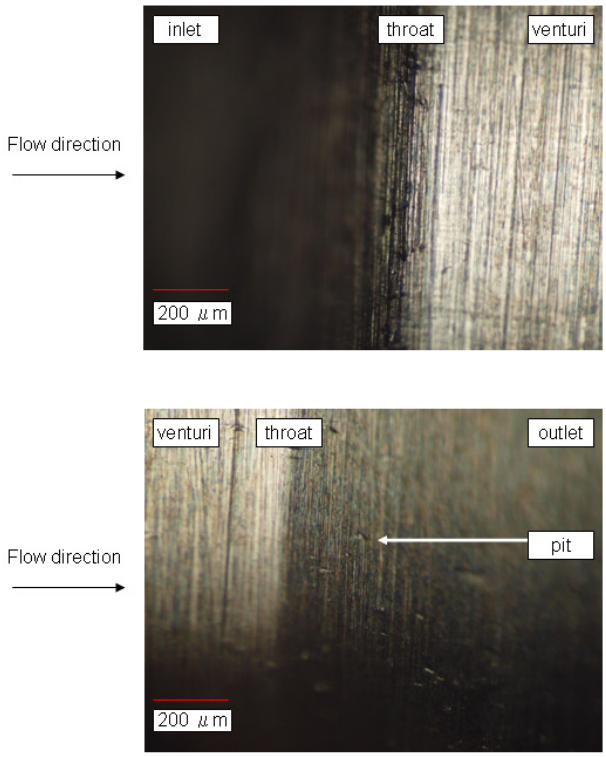

Figure 15. Photograph of the material's surface at inlet (upper photo) and outlet (lower photo) of the venturi.

In order to observe the surface using SEM, the test section was cut into several parts. Observation of the material surface at downstream part of the venturi test section indicates some pits which are dispersed with radius around 50 μm. The number of pits at downstream part of the test section is relatively larger than at the upstream and venturi parts of the test section. This condition occurs because most of the cavitation bubbles collapse at the downstream than any other parts.

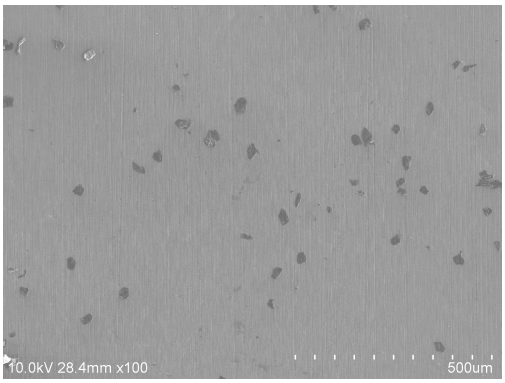

Figure 16. SEM of downstream part of the venturi test section.

8. CONCLUSION

Cavitation experiments to determine the characteristics of cavitation and erosion were carried out in the flowing liquid sodium. The onset cavitation conditions (onset velocities) in liquid sodium are influenced by the change of the stagnant pressure at the expansion tank. Cavitation noise signals at developed cavitation condition are not affected by the change of the stagnant pressure and might be caused by choking of the sodium flow that restricts the formation of cavitation bubbles. For all the different stagnant pressures and temperatures, the onset cavitation coefficient K is around unity.

Erosion experiment for 600 hours reveals that cavity bubbles produce some micro pits at the outlet of the venturi. These pits indicate that erosion is occurred on the surface of the material caused by the collapse of cavity bubbles.

9. ACKNOWLEDGEMENT

This study is financially sponsored by the Japan Nuclear Energy Safety Organization (JNES).

10. NOMENCLATURE

K : Cavitation coefficient
P_0 : Static pressure at downstream
P_1 : Static pressure at venturi part
V_0 : Liquid sodium velocity at downstream region
V_1 : Liquid sodium velocity at venturi region
ρ : Liquid sodium density at given temperature

11. REFERENCES

[1] Thiruvengadam, A., Preiser, H. S. and Rudy, S. L., 1965, "Cavitation Damage in Liquid Metals", *NASA CR-54459, Technical Progress Report 467-3*, HYDRONAUTICS, Inc., Laurel, Maryland.

[2] Hattori, S., Yada, H., Kurachi, H. and Tsukimori, K., 2009, "Effect of Liquid Metal Composition and Hydrodynamic Parameters on Cavitation Erosion", *Wear* **267**, pp. 2033-2038.

[3] Garcia, R. and Hammitt, F. G., 1967, "Cavitation Damage and Correlations with Material and Fluid Properties", *Journal of Basic Engineering* **89** (4), pp. 753-763.

[4] Young, S. G. and Johnston, J. R., 1970, "Effect of Temperature and Pressure on Cavitation Damage in Sodium", *Characterization and Determination of Erosion Resistance, ASTM STP* **474**, pp. 67-108.

[5] Belahadji, B., Franc, J. P. and Michel, J. M., 1991, "A Statistical Analysis of Cavitation Erosion Pits", *Journal of Fluids Engineering* **113**. pp. 700-706.

[6] Ardiansyah, T., Takahashi, M., Yoshizawa, Y., Nakagawa, M., Miura, K. and Asaba, M., 2008, "Acoustic Noise and Onset of Sodium Cavitation in Venturi", *Proceedings of the 6th Japan-Korea Symposium on Nuclear Thermal Hydraulics and Safety* (in CD), Okinawa, Japan.